Supporting Information for "Numerical Investigation of Observational Flux Partitioning Methods for Water Vapor and Carbon Dioxide"

Einara Zahn[1], Khaled Ghannam[2,3], Marcelo Chamecki[4], Arnold Moene[5],

William P. Kustas[6], Stephen Good[7], Elie Bou-Zeid[1]

[1]Department of Civil and Environmental Engineering, Princeton University, Princeton, New Jersey, USA

[2]Program in Atmospheric and Oceanic Sciences (Cooperative Institute for Modeling the Earth System), Princeton University, Princeton NJ, USA

[3]Department of Civil and Environmental Engineering, Northeastern University, Boston, MA

[4]Department of Atmospheric & Oceanic Sciences, University of California in Los Angeles, Los Angeles, California, USA

[5]Meteorology and Air Quality Group, Wageningen University and Research, Wageningen, The Netherlands

[6]USDA-ARS, Hydrology and Remote Sensing Lab, Beltsville, MD 20705-2350, USA

[7]Department of Biological and Ecological Engineering, Oregon State University, Corvallis, OR 97331, USA

Contents of this file

1. Figures S1 to S17

1. Mean wind and kinetic energy across domains

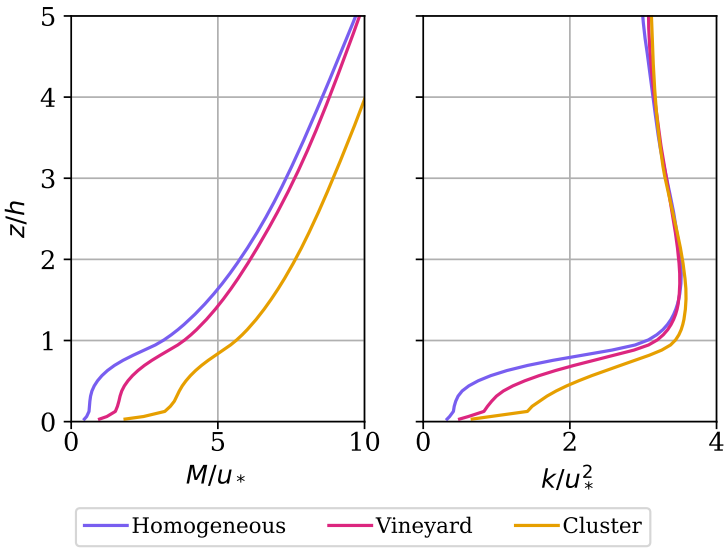

Figure S1. Mean wind $M = (U^2+V^2)^{1/2}$ (a) and kinetic energy profiles (b) across the different domains.

2. Variability across towers

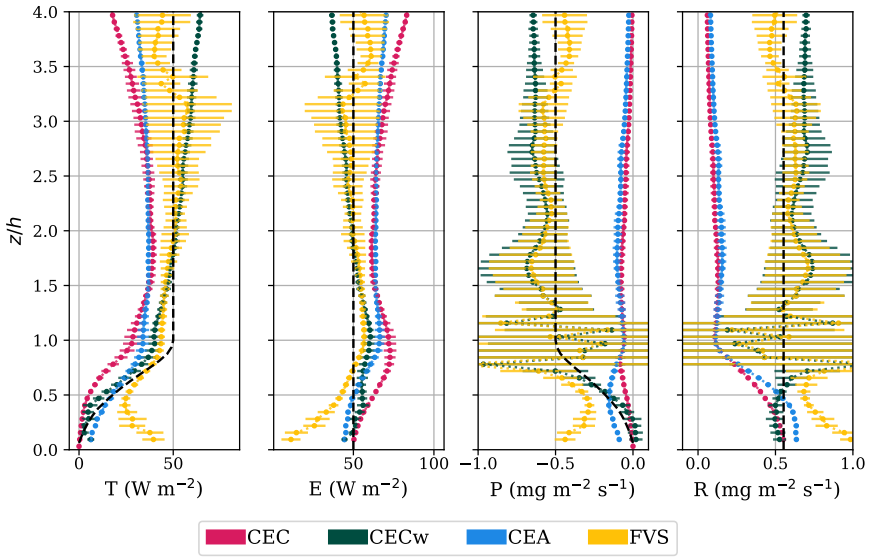

Figure S2. Averaged flux profiles found by CEC, CECw, CEA, and FVS. Bars represent one standard deviation from the mean computed across all 24 towers at every level z.

3. Performance of Partitioning methods over a vineyard-like domain

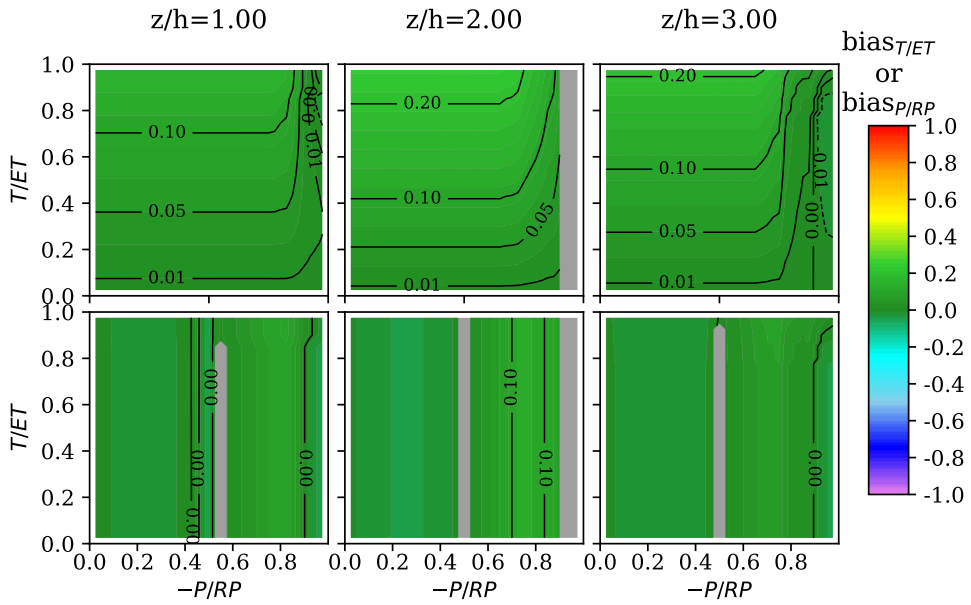

Figure S3. The top three plots show the bias in the partitioning of ET following the FVS method at $z/h = 1, 2, 3$, where the colors represent the bias in transpiration, $(T - T_{CEC})/ET$. Bottom plots show the bias for CO_2 components, defined as $(P - P_{CEC})/PR$, where $PR = R + |P|$. Regions in gray represent combinations when no physical solutions were found. Results over a vineyard-like domain.

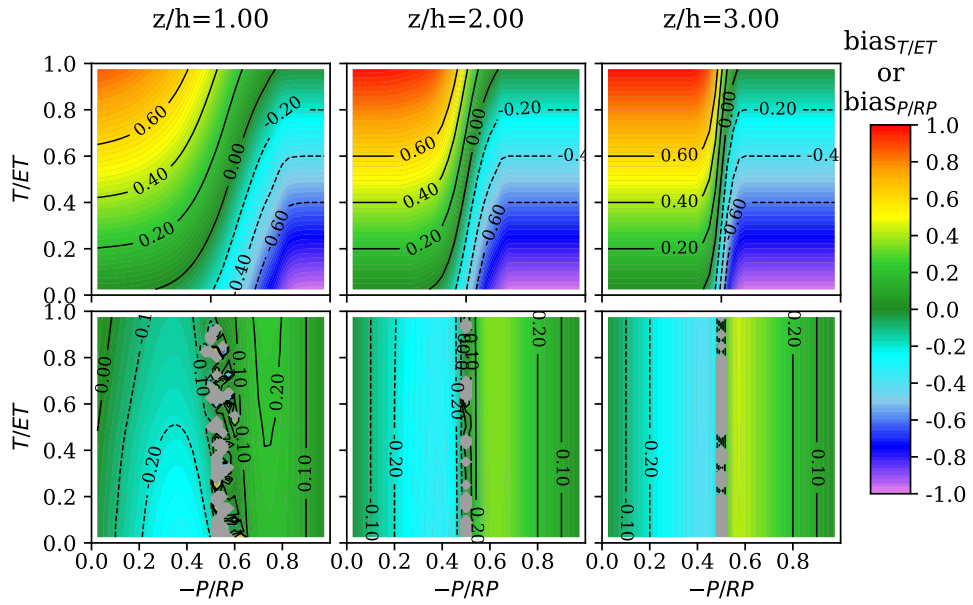

Figure S4. Same as Figure S3, but for the CEC method.

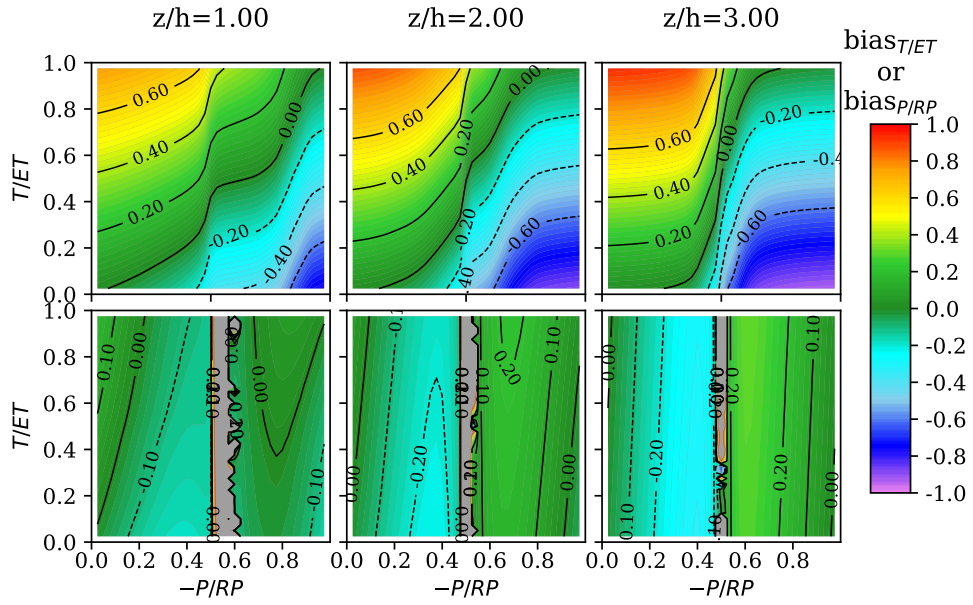

Figure S5. Same as Figure S3, but for the CEA method.

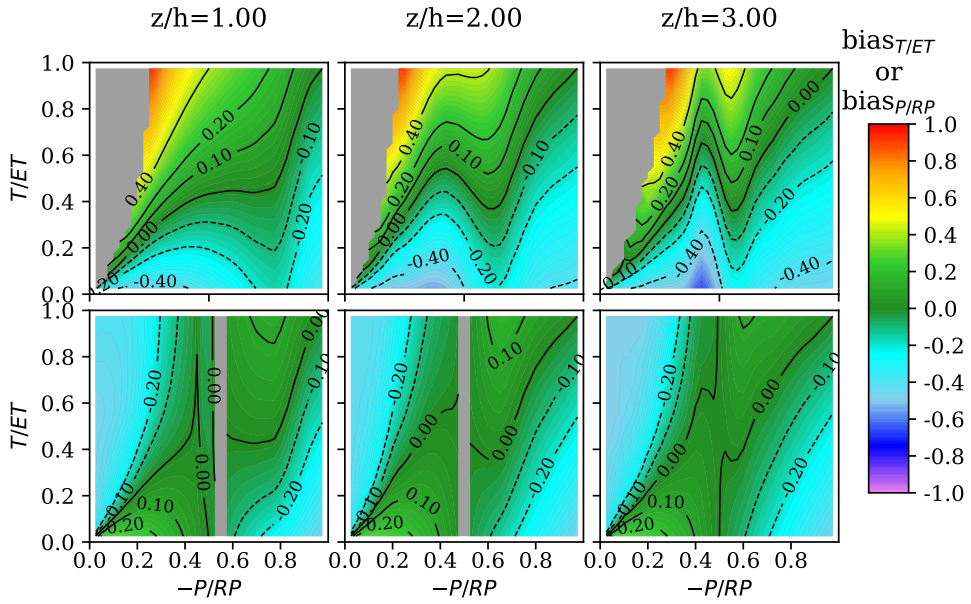

Figure S6. Same as Figure S3, but for the CECw method.

4. Performance of Partitioning methods over a cluster-like domain

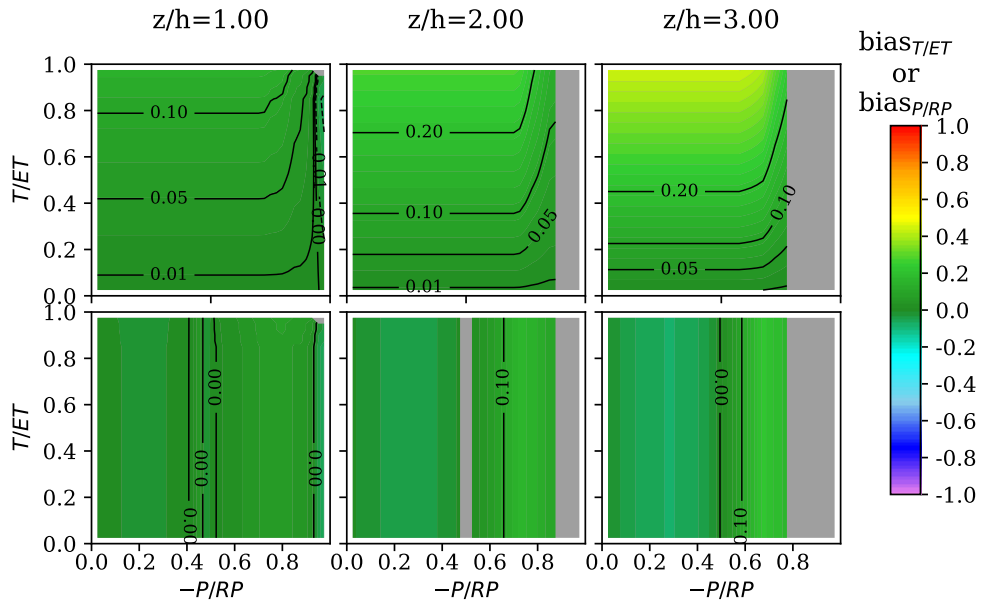

Figure S7. The top three plots show the bias in the partitioning of ET following the FVS method at $z/h = 1, 2, 3$, where the colors represent the bias in transpiration, $(T - T_{CEC})/ET$. Bottom plots show the bias for CO_2 components, defined as $(P - P_{CEC})/PR$, where $PR = R + |P|$. Regions in white represent periods when no physical solutions were found. Results over a cluster-like domain.

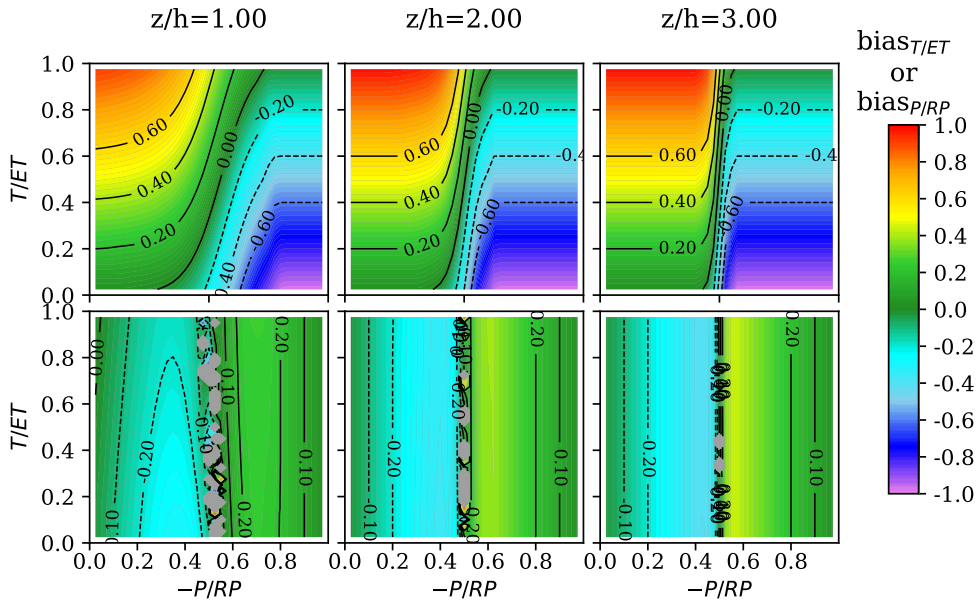

Figure S8. Same as Figure S7, but for the CEC method.

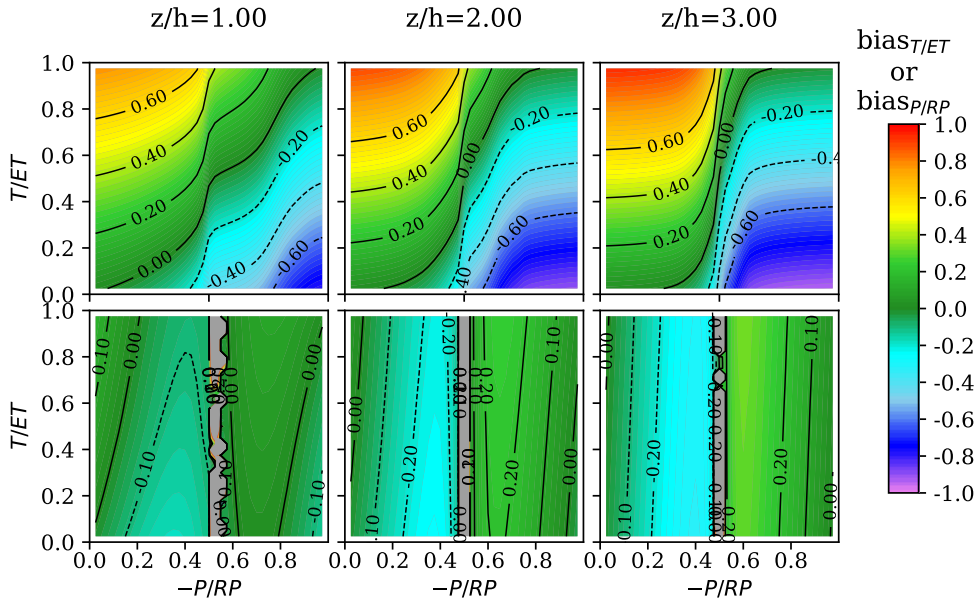

Figure S9. Same as Figure S7, but for the CEA method.

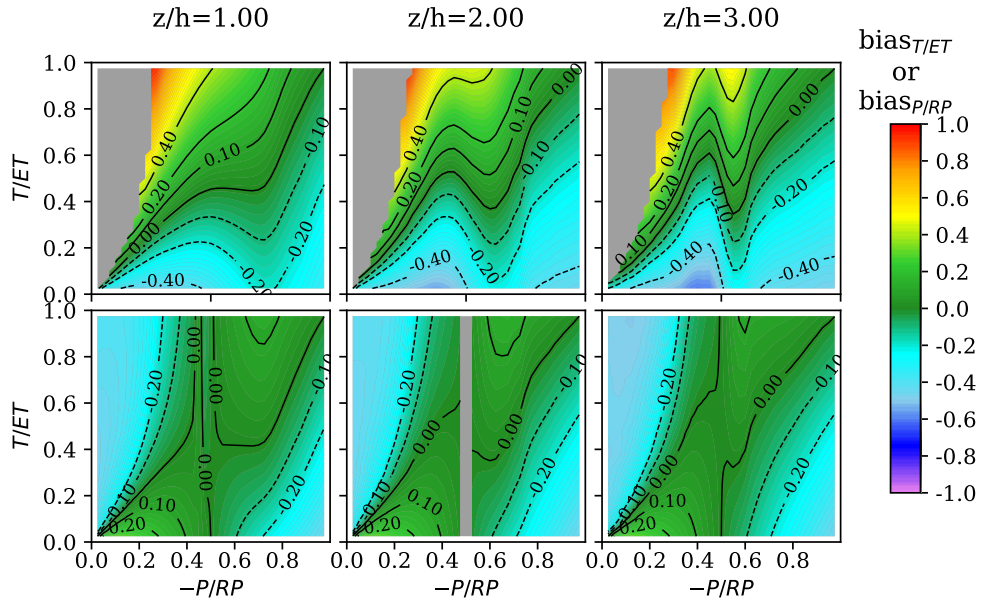

Figure S10. Same as Figure S7, but for the CECw method.

5. Instantaneous fields of CO_2 components over heterogeneus domains

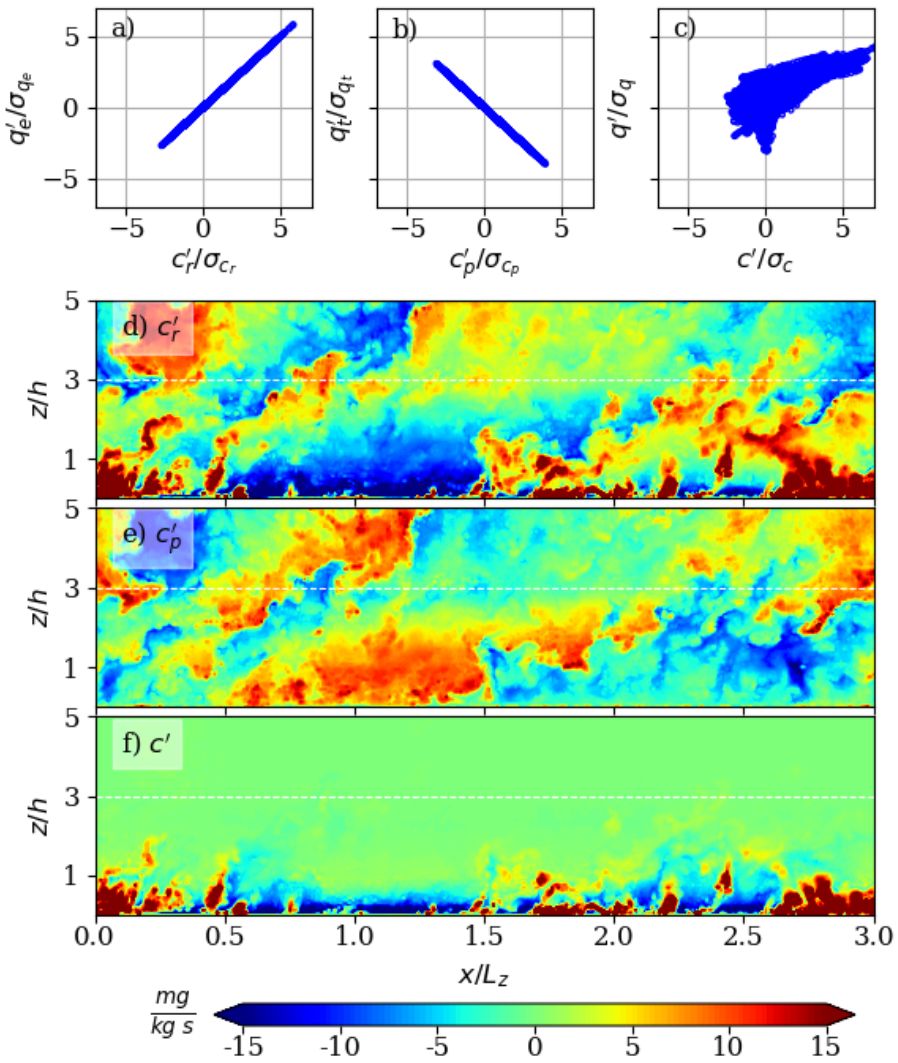

Figure S11. Vineyard-like canopy. Panels a-c show the quadrant plot between the different components of c and q from a time series measured at $z/h \approx 1.2$. Only ejections ($w' > 0$) are included. Note that the conditional sampling implemented by the MREA and CEC is based on plot c). The bottom three panels show instantaneous fields of d) c_r', e) c_p', and (f) $c' = c_r' + c_p'$. The white dashed line represents the height $z = 3h$. In this neutral simulation over a vineyard-like canopy, $R = -P = 1$ mg kg^{-1}s^{-1}.

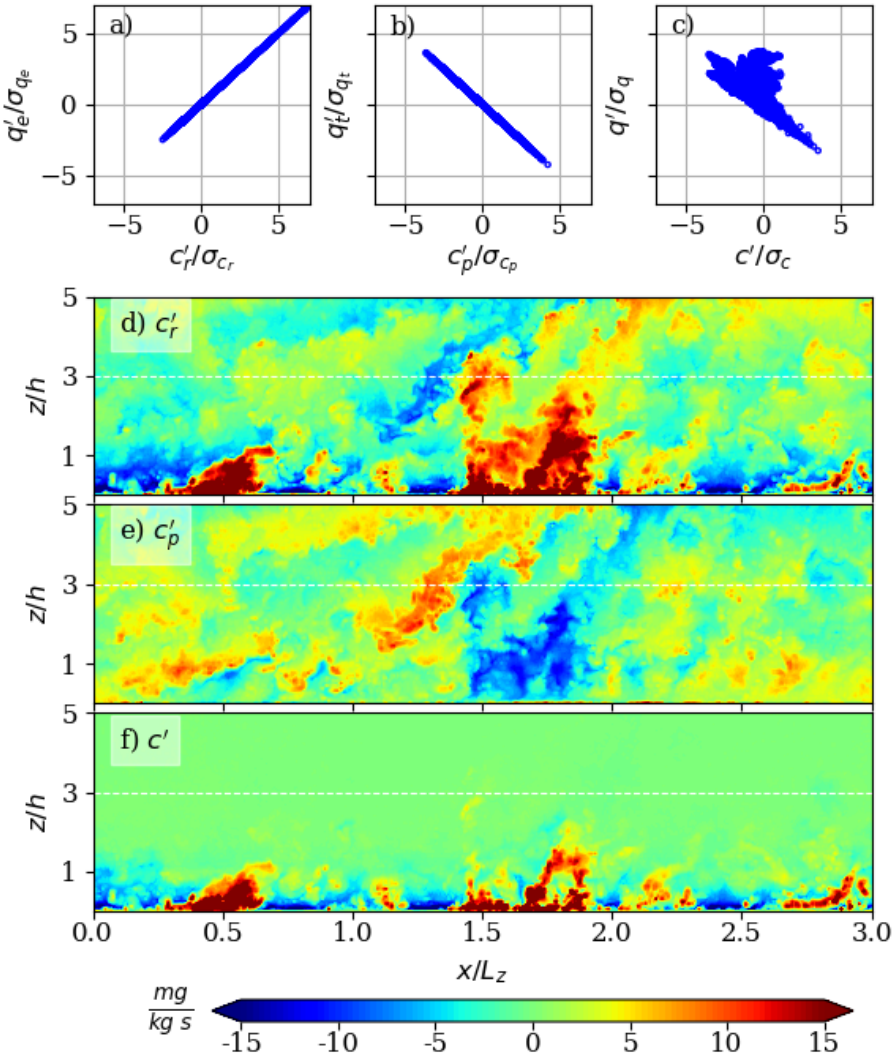

Figure S12. Same as S11, but over a cluster-like canopy.

6. Frequency of valid solutions for the FVS method

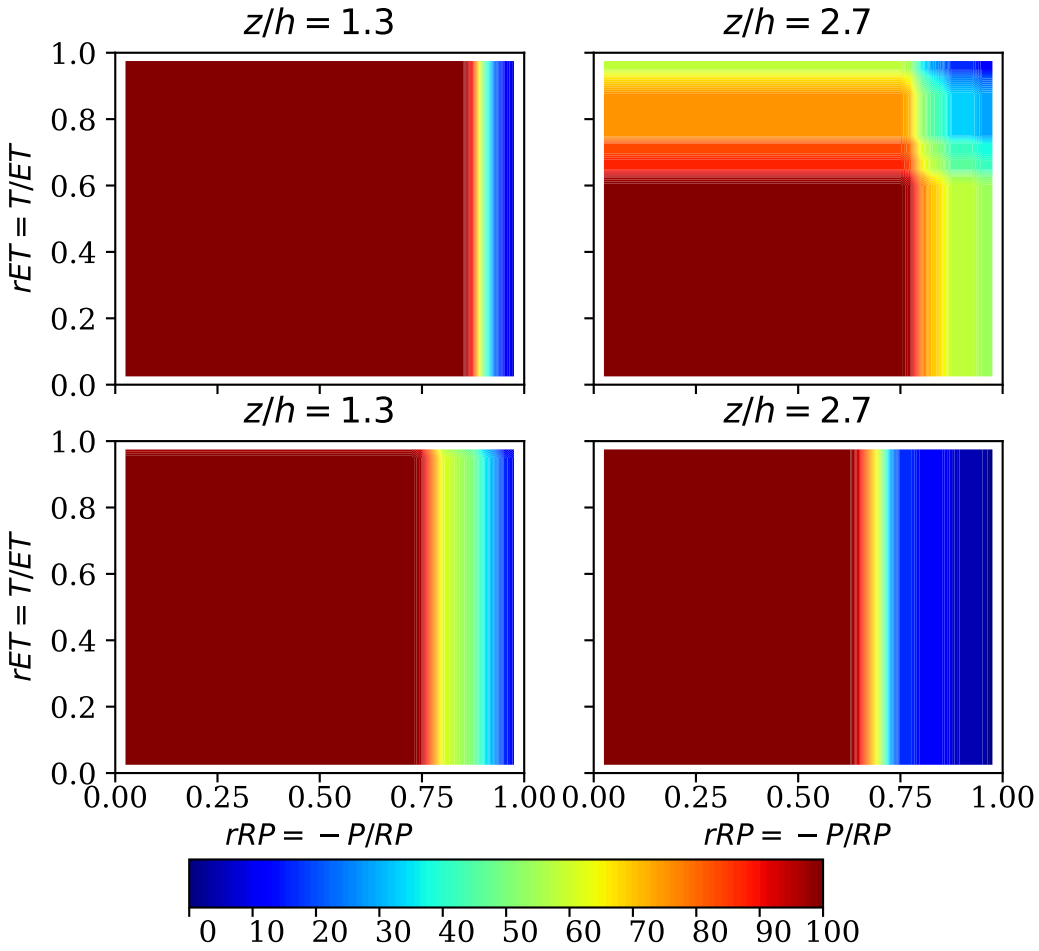

Figure S13. Percentage of valid solutions found by the FVS method at two heights (z/h=1.5 and 3.1) over the homogeneous canopy (top figures) and heterogeneous canopy with clustered vegetation (bottom figures). At each level, FVS was implemented across all 24 towers (time series). The colorbar represents the percentage of valid solutions that were found for the various combinations of flux components (i.e., 100% means that all 24 towers produced valid solutions).

7. Relation between water-use efficiency and correlation coefficient using experimental data

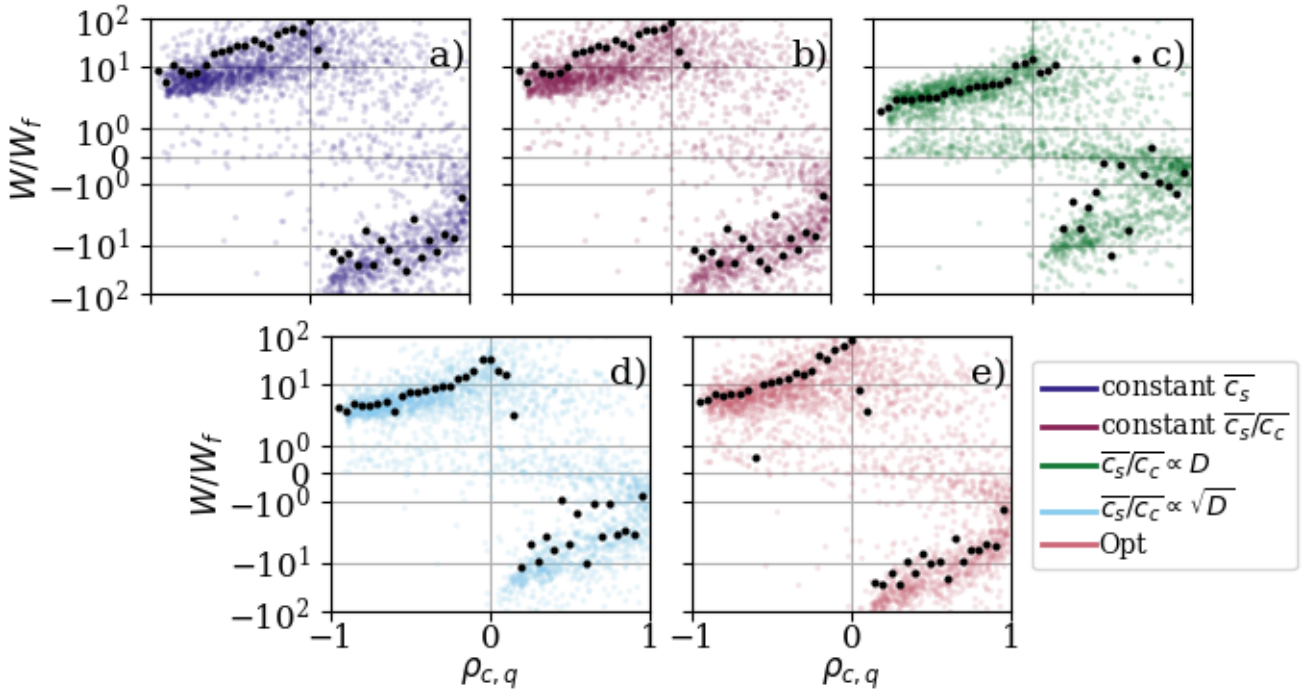

Figure S14. Scatter plot of the ratio W/W_f versus $\rho_{c,q}$ at the NEON site Bonanza Creek (BONA), where $W_f = F_c/ET$. Black markers show the average over intervals $\Delta\rho_{c,q} = 0.05$. Data measured in Spring of 2018 and 2019, only for unstable conditions (*i.e.*, positive heat flux) and when W from all models were available are shown. Each plot represents a different parameterization of the water-use efficiency, more specifically the parameterization of the interstomatal CO_2 concentration, $\overline{c_s}$. The models assume a) constant $\overline{c_s}$, b) constant ratio between interstomatal and near canopy CO_2 concentration, $\overline{c_s}/\overline{c_c}$, c) the ratio $\overline{c_s}/\overline{c_c}$ is linearly proportional to vapor-pressure deficit (D), d) the ratio $\overline{c_s}/\overline{c_c}$ is linearly proportional to $\sqrt{D}$, e) the optimization model proposed by (Scanlon et al., 2019). More details of each model in (Zahn et al., 2022).

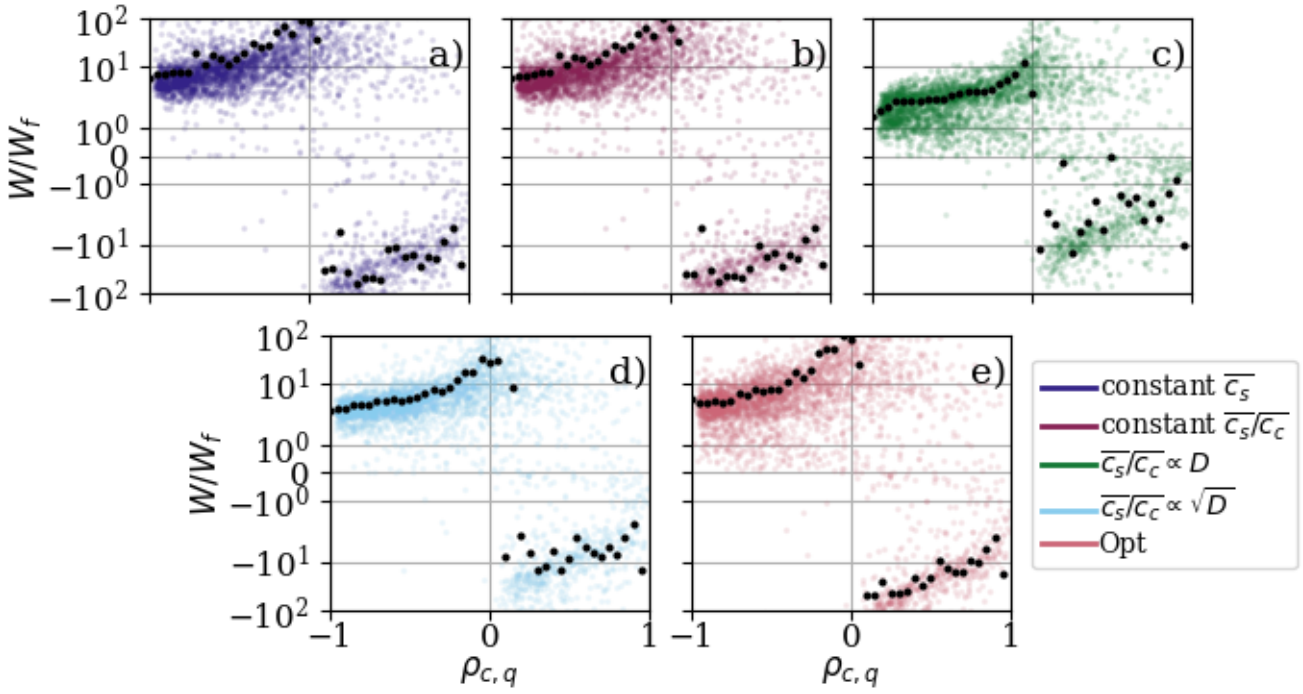

Figure S15. Same as S14, but for the NEON site Delta Junction (DEJU).

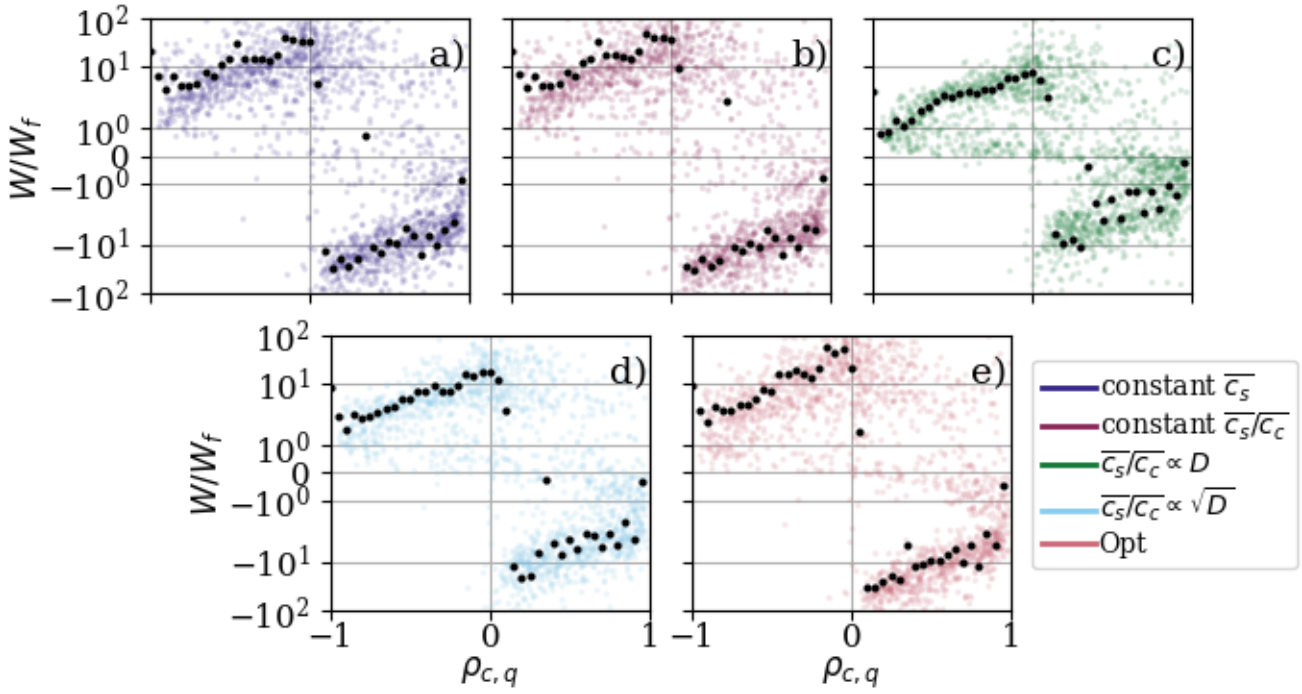

Figure S16. Same as S14, but for the NEON site Harvard forest (HARV).

8. Comparing partitioning methods above a grass field

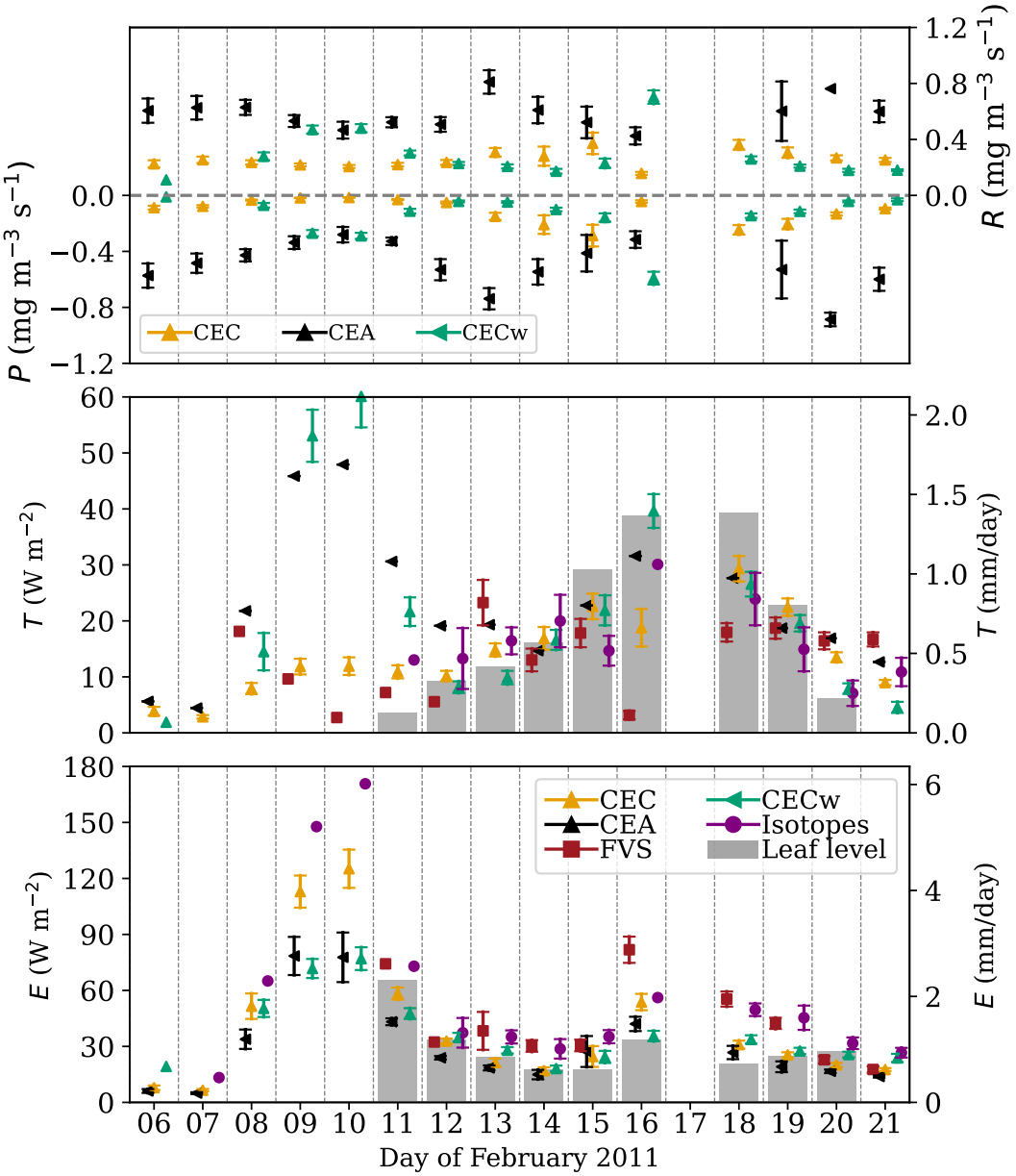

Figure S17. Daily average of partitioning components above a grass site in Kenya, where P and R are shown in the top panel, transpiration in the mid panel, and evaporation in the third panel. A description of the dataset and data processing can be found in (Zahn et al., 2022).

References

Scanlon, T. M., Schmidt, D. F., & Skaggs, T. H. (2019). Correlation-based flux partitioning of water vapor and carbon dioxide fluxes: Method simplification and estimation of canopy water use efficiency. *Agricultural and Forest Meteorology*, *279*, 107732. Retrieved from http://www.sciencedirect.com/science/article/pii/S016819231930348X doi: https://doi.org/10.1016/j.agrformet.2019.107732

Zahn, E., Bou-Zeid, E., Good, S. P., Katul, G. G., Thomas, C. K., Ghannam, K., ... Kustas, W. P. (2022). Direct partitioning of eddy-covariance water and carbon dioxide fluxes into ground and plant components. *Agricultural and Forest Meteorology*, *315*, 108790. Retrieved from https://www.sciencedirect.com/science/article/pii/S0168192321004767 doi: https://doi.org/10.1016/j.agrformet.2021.108790